Invited Paper

# Application of Superresolution Algorithm to Optical Coherent Imaging

J.R. Fienup, M.R. Kosek, and H.C. Stankwitz

Environmental Research Institute of Michigan
P.O. Box 134001, Ann Arbor, MI 48113-4001
Internet: fienup@erim.org

## ABSTRACT

The Super-SVA algorithm has been shown effective for improving the resolution of microwave synthetic-aperture radar (SAR) images.[1] In this paper we review the Super-SVA algorithm and demonstrate its application to optical imaging systems using coherent laser illumination. Examples of such imaging systems include heterodyne-array imaging, holographic laser radar, laser synthetic-aperture radar, coherent phase retrieval from pupil-plane intensities, and SCIP (sheared-beam imaging). We consider the case of a bright object on a dark background. We show the difference in performance for different features of the image -- prominent points versus extended, diffuse areas.

**Keywords**: Super-resolution, coherent imaging, image processing, sidelobes, bandwidth extrapolation, iterative algorithm

## 1 INTRODUCTION

The resolution of optical imagery is classically limited by diffraction from the collecting aperture. For many years researchers have sought signal-processing and mathematical approaches to recovering greater detail from collected imagery. Recently a new superresolution technique, Super-SVA,[1] has proven successful for obtaining improved resolution from microwave synthetic-aperture radar (SAR) imagery. In part, it is effective there because, at long wavelengths, cultural objects are highly specular, making point-like scatterers common in microwave SAR. In this paper we explore the efficacy of Super-SVA to optical imagery. This would be applicable to coherent imaging modalities such as heterodyne-array imaging, holographic laser radar[2] laser synthetic-aperture radar,[3] coherent phase retrieval from pupil-plane intensities,[4] and SCIP (sheared-beam imaging),[5] among others. It can also be applied to non-optical imaging modalities governed by a coherent transfer function, such as magnetic resonance imaging (MRI). For these imaging modalities the impulse response is the Fourier transform of the aperture function, rather than the squared magnitude of the Fourier transform of the aperture function.

Even though the coherent optical imaging process may be mathematically equivalent to the SAR imaging process, the superresolution algorithm may not work as well because of the nature of the optical imagery. In particular, at optical wavelengths, objects are less specular, resulting in fewer, if any, point-like image features that are important to the success of Super-SVA. In this paper we show examples of simulated coherent optical images and demonstrate the effectiveness of Super-SVA in obtaining additional resolution from them. We show the difference between objects having specular components and those that are purely diffuse. We begin by reviewing Super-SVA, then show results for the two types of optical images, and discuss the results.



0-8194-2215-0/96/$6.00

## 2 SVA AND SUPER-SVA

Before describing Super-SVA, we briefly describe the spatially variant apodization (SVA) algorithm,[6] the engine that makes it work.

Sidelobes of the impulse response in an image can be controlled by placing a weighting or apodization function over the aperture. However, while weighing down the edges of the aperture does decrease sidelobes, it does so at the expense of widening the main lobe of the impulse response, thereby degrading resolution. SVA circumvents this trade-off, yielding an image of a point source having the fine resolution of an unweighted aperture while having no sidelobes whatsoever. It accomplishes this feat by effectively computing the images from a family of aperture weighting functions, and selecting, on a pixel-by-pixel basis, the image value having the minimum magnitude. Because of the properties of the cosine-on-a-pedestal weighting functions — which includes unweighted, Hamming, and Hanning functions as special cases — this minimization can be done very simply and efficiently from the image computed from an unweighted aperture. The special property that makes this efficiency possible is the fact that the discrete Fourier transform of these weighting functions consists of only three non-zero pixels: the center pixel and two adjacent sidelobe pixels, the values of which are proportional to the coefficient of the weighting function. Hence the images from all the other members of the family of weighting functions can be computed by a simple three-point convolution. We can do this in analytic form and arrive at an expression for the intensity of any given pixel as a function of the weighting-function coefficient. We can also analytically solve for the value of the coefficient that minimizes the intensity at a given pixel. Hence we can efficiently select, on a pixel-by-pixel basis, the weighting function that minimizes the sidelobes at each pixel. The result is a preservation of the narrowest mainlobe from the family of weighting functions but the elimination of sidelobes,[6] as illustrated in Figure 1 for an image consisting of a single point scatterer.

We see from Figure 1(c) that the result of SVA, in eliminating the sidelobes while preserving the fine-resolution main lobe, is to produce an image that has discontinuous first derivatives. These discontinuities cause the Fourier transform of the SVA image to have energy outside the area of the original aperture, and differ somewhat from the measured data within the original aperture.

These ingredients are all analogous to those employed for the Gerchberg super-resolution algorithm.[7] For the Gerchberg algorithm we assume that the object being imaged is of finite extent, so we truncate the image to that finite extent, causing a discontinuity that introduces higher-frequency data into its Fourier transform. Then we replace the Fourier transform of that image with the measured Fourier data within the area of the aperture, while keeping the new information at the higher spatial frequencies. We then recompute the image from this extended Fourier transform and repeat the process.

At its most basic level, the Super-SVA algorithm is a modified version of the Gerchberg algorithm, replacing the image-domain support-constraint (truncation) operation by the SVA sidelobe-elimination operation. As iterations progress, more and more energy is added at the higher spatial frequencies outside the aperture, thereby extrapolating the aperture, and achieving improved resolution in the image. Additional details can be found in Reference 1. Super-SVA is effective because SVA injects discontinuities throughout the image rather than just at the edges of the image, thereby creating higher spatial-frequency information in a highly effective manner.

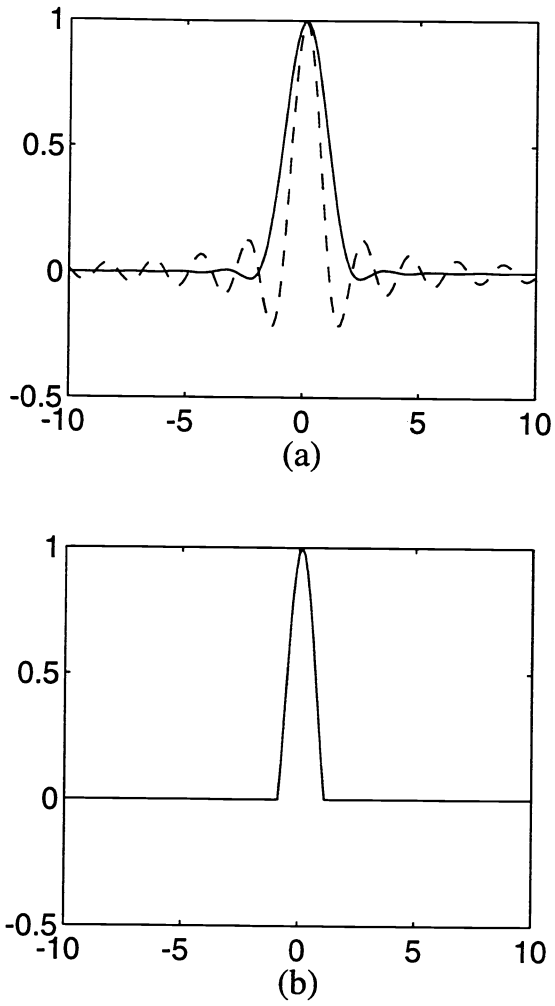


Figure 1. Image of a Point. (a) From unweighted aperture (dashed line) and from Hanning-weighted aperture (solid line), (b) after SVA.

## 3 SUPER-SVA FOR OPTICAL IMAGERY

Super-SVA works well for microwave SAR imagery, in which bright, point-like scatterers are common. The question that concerns us here is how well might it work for coherent optical imagery, for which specular returns are less common, and sometimes are entirely absent. We answer this question by computer simulation experiments. We start with an incoherent optical image of an object, simulate realizations of speckled, coherent imagery of the object, run Super-SVA, and examine the results. Since subtle details are difficult to discern from a single speckled image, we noncoherently average many images together to reduce the speckle artifacts and more readily discern the difference between the images before and after Super-SVA.

Figure 2 shows the results for our first test object, a photograph of a model of a satellite. This object, made of optically shiny materials, has substantial specular reflections as well as a diffuse component. Figure 2(a) shows the object model. We simulated 36 realizations of coherent speckled

images, each obtained by multiplying the square root of the object by a pure-phase function having a different random phase, then low-pass filtering using a square aperture of length 32 pixels in the Fourier domain. Individual speckled images are difficult to interpret, so we show in each case the noncoherent average of all 36 speckle realizations. The averaging reduces (but does not eliminate) the speckle artifacts. Figure 2(b) shows the original diffraction-limited averaged image, computed from an unweighted aperture. Figure 2(c) shows the averaged image when Taylor weighting was applied to the apertures. It reduces the sidelobes, but at the expense of degraded resolution. Figures 2(d) shows the result of SVA, which has the fine resolution of the image from the unweighted aperture, but without the sidelobes. Figure 2(e) shows the result of Super-SVA, attempting a doubling of the resolution. For comparison we show, in Figures 2(f), the averaged images from an aperture of length 64 pixels, giving true twice-resolution. Comparing 2(e) with 2(b) and 2(f), we see that the Super-SVA image does have finer detail than the original image; and that in the specular point-like areas of the image, the finer detail matches that of the true finer-resolution image. For the diffuse portions of the image, the improvements obtained by Super-SVA are modest, and certainly do not achieve the factor of two improvement seen in the point-like areas of the image.

Figure 3 shows the same things for our second object, a CAD-CAM image of a missile that has no specular returns. Again, SVA greatly reduces the sidelobes, thereby removing the haze in the image around the object. This is a much more difficult case for Super-SVA or for any other superresolution algorithm. In this case, the Super-SVA image does look somewhat sharper than the original diffraction-limited image, but at the price of increasing contrast of the residual speckles in the image. In particular, the point of the missile in the upper-left corner appears sharper than in the original image. The details in the area of the fins in the lower right corner appear slightly sharper as well. However, these effects are subtle enough that they might be difficult to discern in the image reproduced on the page.

Figure 4 shows averaged cuts through the center region of the 32 noncoherently averaged images. The cuts reveal the width of the target. To get a better feel for the width, and to further reduce the effect of the speckles, we averaged over 75 parallel cuts through the center of the image, each shifted appropriately to line up the center of the missile. The top dotted curve shows the given image, with no aperture weighting. The third-from-top dashed curve shows the result of SVA, which is considerably narrower, a marked improvement. The fourth-from-top solid curve shows the result of Super-SVA, a still greater improvement. For comparison, the second-from-top dash-dot curve shows the averaged cuts through the true twice-finer-resolution image (no aperture weighting), and the lowest dotted curve shows the result of SVA on the true twice-finer resolution image. The Super-SVA algorithm reveals an apparent object width that is more consistent with the true twice-finer-resolution image.

## 4 CONCLUSIONS

We show that SVA and Super-SVA, originally developed for microwave synthetic-aperture radar, also work well for coherent optical imagery. We found that, in the diffuse areas of an image, SVA yields a considerable improvement in image quality over a conventional image, and Super-SVA yields a slight additional improvement. In the specular areas of the image, SVA yields a considerable improvement in image quality over a conventional image, and Super-SVA yields a considerable additional improvement, resulting in a factor-of-two improvement in resolution. Further testing will be required to determine the effects of noise.

On the basis of these results, we recommend the use of Super-SVA on a wide variety of imagery from systems with coherent transfer functions.

## ACKNOWLEDGMENTS

This work was supported by the Innovative Science and Technology directorate of the Ballistic Missile Defense Organization, through the Naval Command, Control, and Ocean Surveillance Center RDT&E Division (NCCOSC/NRaD) and the Naval Air Warfare Center (NAWC)

## REFERENCES

1. H.C. Stankwitz and M.R. Kosek, "Super-Resolution for SAR/ISAR RCS Measurement Using Spatially Variant Apodization," Proceedings of the Antenna Measurement Techniques Association (AMTA) 17th Annual Meeting and Symposium, Williamsburg, VA, 13-17 November 1995.

2. J.C. Marron and K.S. Schroeder, "Three-dimensional Lensless Imaging Using Laser Frequency Diversity," Appl. Opt. 31, 255-262 (1992).

3. C.C. Aleksoff, J.S. Accetta, L.M. Peterson, A.M. Tai, A. Klooster, K.S. Schroeder, R.M. Majewski, J.O. Abshier, and M. Fee, "Synthetic Aperture Imaging with a Pulsed $CO_2$ TEA Laser," in Laser Radar II, Proc. SPIE 783, 29-40 (1987).

4. J.R. Fienup, "Reconstruction of a Complex-Valued Object from the Modulus of Its Fourier Transform Using a Support Constraint," J. Opt. Soc. Am. A 4, 118-123 (1987).

5. R.A. Hutchin, "Sheared Coherent Interferometric Photography: A Technique for Lensless Imaging," in digital Image Recovery and Synthesis II, Proc. SPIE 2029, 161-168 (1993).

6. H.C. Stankwitz, R.J. Dallaire, and J.R. Fienup, "Non-linear Apodization for Sidelobe Control in SAR Imagery," IEEE Trans. AES 31, 267-278 (1995).

7. R.W. Gerchberg, "Super-Resolution through Error Energy Reduction," Optica Acta 21, 709-720 (1974).

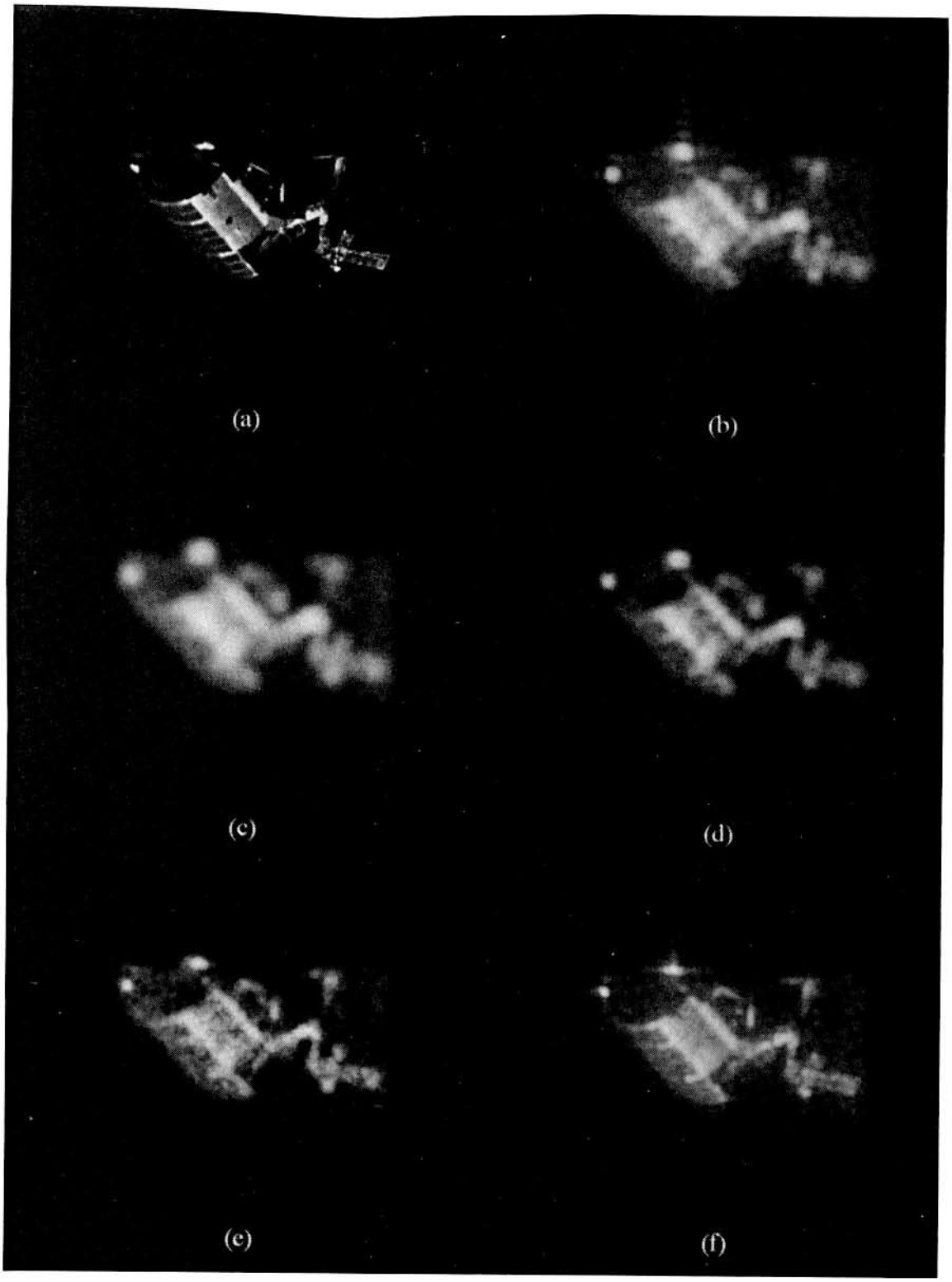


Figure 2. SVA and Super-SVA for Semi-Specular (Satellite) Object. (a) Object model, (b) diffraction-limited image from unweighted aperture, (c) image from Taylor-weighted aperture, (d) result of SVA, (e) result of Super-SVA, (f) image with twice-finer resolution.

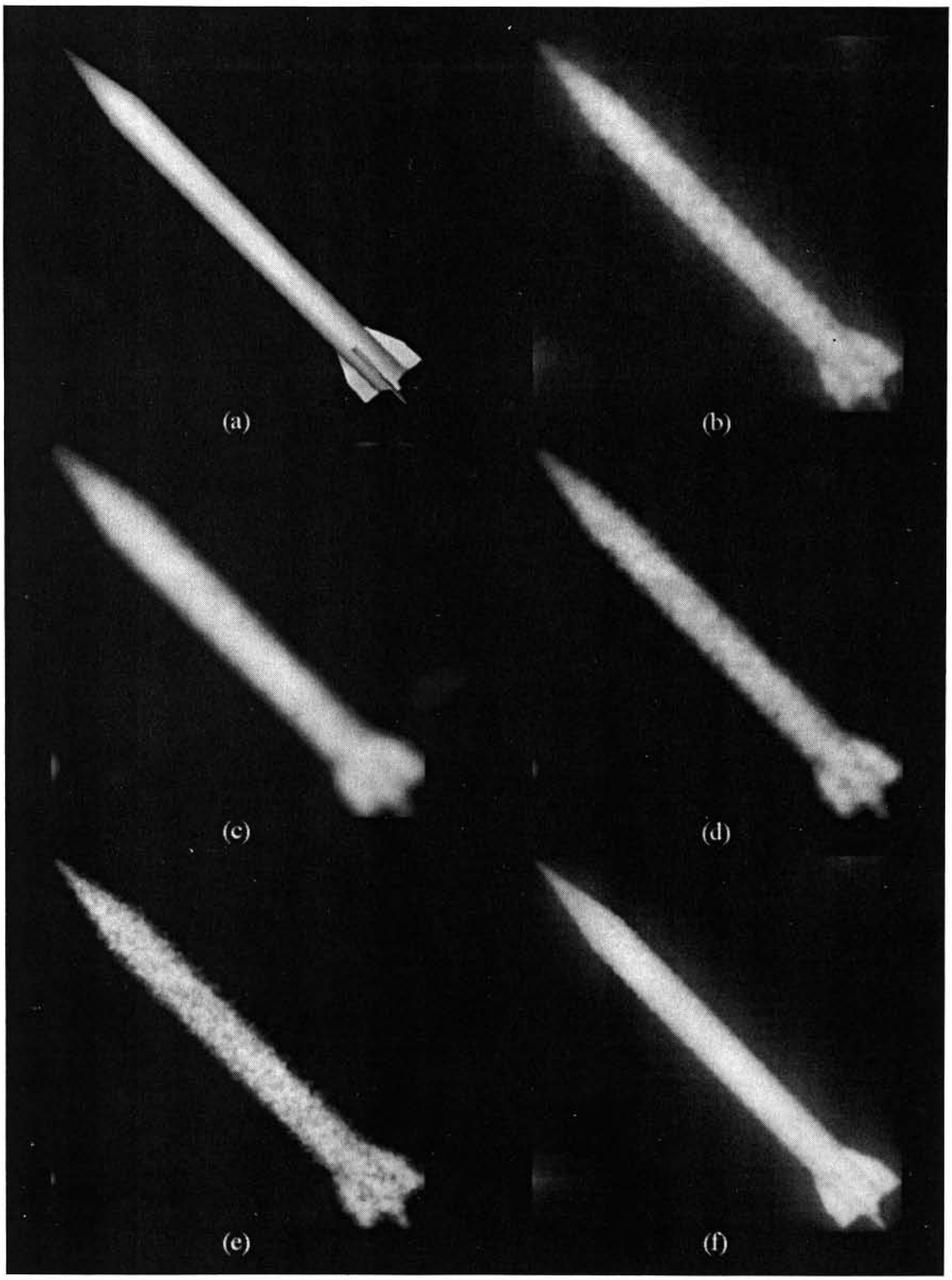


Figure 3. SVA and Super-SVA for Diffuse (Missile) Object. (a) Object model, (b) diffraction-limited image from unweighted aperture, (c) image from Taylor-weighted aperture, (d) result of SVA, (e) result of Super-SVA, (f) image with twice-finer resolution.

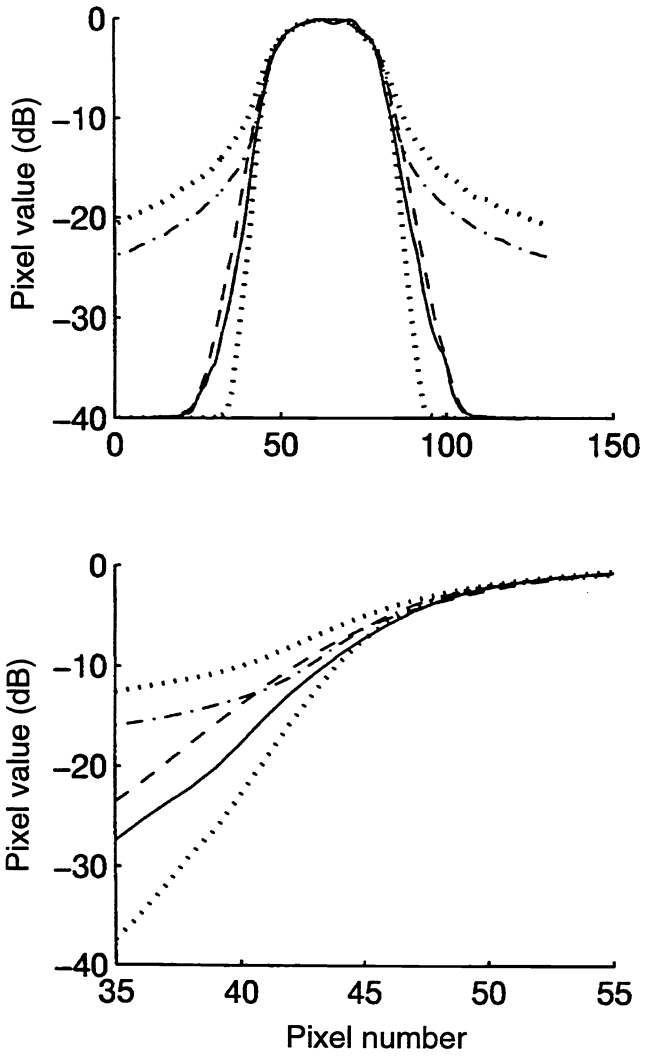


Figure 4. Averaged Cuts through the Missile Image (Log Plots). (a) Over entire width of object; (b) Of left edge of object. Curves (top-to-bottom) represent the given image (····), the true twice-finer resolution image (–·–·), SVA on the original image (– –), Super-SVA on the original image (—), and SVA on the true twice-finer-resolution image (····).